Non-thrombogenic hydrogel coatings with carbene-crosslinking bioadhesives

Himansu Sekhar Nanda[1,2,+], *Ankur Harish Shah*[1,+], *Gautama Wicaksono*[1], *Oleksandr Pokholenko*[1], , *Feng Gao*[1], *Ivan Djordjevic*[3], *Terry W. J. Steele*[1,*]

[1] School of Materials Science and Engineering, Nanyang Technological University, 50 Nanyang Avenue, Singapore 639798

[2] Department of Mechanical Engineering, PDPM-Indian Institute of Information Technology, Design and Manufacturing (IIITDM)-Jabalpur, Dumna Airport Road**,** Jabalpur-482005, MP, India

[3]Tecnologico de Monterrey, School of Engineering and Sciences, Monterrey, NL 64849, Mexico

*wjsteele@ntu.edu.sg

[+] Authors have contributed equally to the manuscript contribution

Keywords: PAMAM-g-diazirine; bioadhesives; platelets; thrombogenic; surface modification

Abstract:

Bioadhesives are a current unmet clinical need for mending of blood contacting soft tissues without inducing thrombosis. Recent development of carbene precursor bioadhesives with the advantages of on-demand curing, tuneable modulus, and wet adhesion have been synthesized by grafting diazirine onto poly (amidoamine) (PAMAM-G5) dendrimers. Herein, the structure activity relationships of platelet adhesion and activation is evaluated for the first time on the cured PAMAM-g-diazirine bioadhesives. Three strategies were employed to prevent healthy human donor platelets from adhering and activating on light cured bioadhesive surfaces: 1) Attenuation of cationic surface charge, 2) anti-fouling composites by incorporating heparin and alginate in uncured formulation, and 3) heparin wash of cured bioadhesive surface. Topographical imaging of cured and ethanol dehydrated bioadhesive surfaces was used to quantify the adhered and activated platelets with scanning electron microscopy, whose resolution allowed identification of round senescent, short dendritic, and long dendritic platelets. Cured surfaces of PAMAM-g-diazirine (15%) had 10300±500 adhered platelets mm^{-2} with 99.7% activation into short/long dendritic cells. Reduction of primary amines by higher degree of diazirine grafting or capping of free amines by acetylation reduces platelet adherence (2400±200 vs. 3000±300, respectively). Physical incorporation of heparin and alginate in the formulations reduced the activated platelet; 1300±300 and 300±50, activated platelets mm^{-2}, in comparison with additive free adhesive formulation. Similarly heparin rinse of the surface of additive free bioadhesive reduced the activated platelet to platelets of heparin composites at 600±100 platelets mm^{-2}. PAMAM-g-diazirine (15%) bioadhesive retained the photocured mechanical properties and lap shear adhesion despite the addition of heparin and alginate additives.

1. Introduction

Tissue adhesives are an unmet clinical need required to seal internal wounds towards a replacement of mechanical fixation methods, e.g. sutures and staples. Ideally, the cured tissue adhesive should match the tissue elasticity and achieve adhesion even on wet substrates. If the adhesive is applied towards blood contacting tissues, the cured adhesive matrix should have little to nothrombogenicity[1]. Thrombogenesis arises after biomaterials (natural or synthetic) are exposed to blood; and is associated with fibrinogen adsorption that induces platelet adhesion, activation or combination thereof[2]. Upon activation, platelets transition into a dendritic morphology and subsequently release positive feedback signals for additional platelets to spread over the biomaterial surface [3, 4]. The positive feedback cycle of degranulation and spreading further recruits additional platelets to cause layers of platelet-platelet interaction, aggregation and thrombus formation [5]. If bioadhesives or tissue adhesives are employed for fixing blood-contacting soft tissues (e.g. artery anastomosis) or prophylactic blood-contacting medical implants (e.g. controlled release depots), platelet adhesion, activation, or combination thereof needs to be minimized. Development of minimally non-thrombogenic tissue adhesives is required towards minimizing the risk of microclots that lead to strokes and infarcts[6 7]. Current commercially available bioadhesives have not been designed in this regard.

Fibrin adhesive (e.g. TISSEEL, Baxter) and polyurethane adhesive (e.g. TissuGlu, Cohera Medical), are used in auxiliary roles to support sutures. TISSEEL, a fibrin based adhesive is biocompatible but weak adhesive and mechanical properties[8-9] limits them to hemostasis applications and therefore cannot be used as a candidate bioadhesive for non-thrombogenic fixation and coatings [10 11]. Polyurethane based adhesives show thrombotic responses[12-13] and also suffer from slow-cure rates (i.e. hours), which limits them to static applications such as abdominoplasty. Thus, synthetic bioadhesives are required that possesses both fast activation and minimally thrombogenic properties.

Most blood contacting biomaterials require some form of surface modification to decrease platelet adsorption, activation, or combination thereof thus making the implant surface platelet resistant [14].

Specific strategies rely on covalent conjugation of an appropriate platelet resistance chemical moiety or by incorporating external anti-fouling additives, such as PEG as described above. Besides PEG, heparin and alginates are additives typically incorporated through physical mixing or adsorption techniques[15-14]. Heparin's anti-thrombogenic attributes are exploited throughcontrolled release or non-eluting technologies that is intended for permanent covalent immobilization to the biomaterial surface [16 17 18]. Similarly, hemocompatible composite coatings were engineered by layer-by-layer adsorption of alginate and heparin, crosslinked together by UV-activated diazonium crosslinkers [19]. This technology shows that platelet resistance of heparin and alginate remains after crosslinking and UV light wasn't detrimental to their utility. However, diazonium crosslinking mechanisms cannot be incorporated into tissue adhesives, as it has poor stability at physiological pH (decomposition) and temperature (explosive)[20-21].

Tissue adhesives based on carbene precursors offers a new platform of adhesive curing with benefits of on-demand curing within seconds, pH stability, wet adhesion, and shear adhesion strengths in the 10's of kPa. Previous publications have successfully grafted the carbene precursor, bromo-diazirine, onto a 5^{th} generation polyamidoamine (PAMAM) dendrimer via nucleophilic alkylation[22, 23]. The cationic tissue adhesive can be cured through UVA light (365 nm) exhibiting dose dependent adhesion strength, tuneable modulus and adhesion on wet organ substrates. The amine ($-NH_2$) functionalities of PAMAM dendrimer allows one-step stoichiometric grafting, but ungrafted free amines are known to induce platelet adhesion and activation [24 25]. Left unmodified, the positively charged primary amines will induce platelet activation and other thrombotic pathways. . To minimize thrombogenesis, three strategies are hypothesized to reduce or prevent platelet adsorption and activation of the UV-cured PAMAM-g-diazirine bioadhesives: 1) Capping of the PAMAM surface amines to reduce or remove cationic charge, with additional diazirine grafting or converting amines to amides. 2) Incorporating anionic heparin or alginate additives to form hydrogel composites whose cationic charge is electrostatically shielded, displays 'stealth effect', or combination thereof. 3) Applying a heparin wash of the post-cured PAMAM-g-diazirine, whereby the heparin electrostatic interaction shields the PAMAM cationic surface charge with immobilized anticoagulant heparin.

These strategies are then objectively evaluated by incubating the cured bioadhesive formulations with platelet rich plasma from healthy human volunteers. Bioadhesive assessment of the composites was performed with real-time photorheology, shear adhesion, and degree of swelling.

2. Experimental: Materials and Methods

2.1 Materials

Poly (amidoamine) (5^{th} generation, Mw=28.8 kDa, **I**) was purchased from Dendritech, USA. 3-[4-(bromomethyl)phenyl]-3-(trifluoromethyl)-diazirine (bromo-diazirine, **II**) was purchased from TCI, Japan. Poly-DL-lactide-co-glycolide (PLGA 53/47), were purchased from Sigma Aldrich, USA. Heparin sodium (injectable grade, Mw=25KDa) was purchased from Yantai Dongcheng Biochemicals, China. Sodium Alginate (Mw= 350 kDa) was purchased from Sigma Aldrich, USA. The deionized (DI) water from ultrapure water purification system (Merck Millipore, USA) was used for buffer preparations.

2 Methods

2.1 Preparation of PAMAM-g-diazirine with capped terminal amines, V

III and **IV (Fig.1a)** were prepared and characterized (**Fig. S1** and **Table S1**) as previously described [22]. **V** was prepared by dissolving **III** (100 mg, 2.9 µmol; 320 µmol $-NH_2$) in 10 mL methanol, and subsequently cooled in an ice/salt water bath. Neat acetyl chloride (CH_3COCl, 200 mg, 2.55 mmol; 8x molar excess) was added dropwise and the temperature of the reaction solution was maintained below 5^oC for 4 h. Methanol was removed as by rotary evaporation and the viscous liquid was stored under high vacuum (< 2 Torr) until a constant weight. Acetylation of **V** was estimated at 73% via ^1H NMR (see supporting information).

2.2 Preparation of cured PAMAM-g-diazirine formulations III to VII

Formulation **III**, **IV**, and **V** (100 mg) were dissolved in 1:1 w/w 1X PBS and vortexed for 10 min to obtain a homogeneous solution. The formulation was pipeted onto an ethanol sterlized 50 µm polyethylene terephthalate sheets and knife casted into a 500 µm uncured adhesive layer. **III** was mixed with 5-15% heparin or 3% alginate solution (PBS buffer) in 1:1 w/w ratio of additive/**III**. The formulations were cured using a UVA 365 nm wavelength Omnicure 1000 lightguide (Excelitas Technologies Corp., USA) with irradiation power of 100 mW cm^{-2} (effective UV dose of 20 J cm^{-2}) to obtain cured PAMAM-g-Diazrine coating on a PET substrate. A control sample of heparin washed PAMAM-g-diazirine (15%) bioadhesive surface was prepared by washing the surface of cured **III** with 5% w/v heparin solution (PBS buffer). Samples were vacuum dehydrated until ready for platelet assessment.

2.3 Photorheometry of PAMAM-g-Diazirine bioadhesives

The UV curing kinetics studies were evaluated on a Anton Parr Physica MCR 501 rheometer equipped with a stationary glass plate (P=PTD120/GL, Anton Paar, Austria) allowing UV irradiation during the measurement. Measurements were performed using moveable 10 mm parallel plate with a measuring gap of 0.1 mm. The 365 nm UVA light was transmitted from a mercury vapor short arc lamp through a light guide (Omnicure S1000). The intensity of the UVA light was measured using a 843-R powermeter (Newport Opto-Electronics (Singapore) Ltd) and set at 100 mW cm^{-2}. The parameter for oscillatory experiments were set at 1 Hz and 1% strain, with measurement performed as function of time, starting with two minutes without irradiation followed by 200 seconds of continuous irradiation for a total UV dose of 20 J cm^{-2}.

2.4 Lap shear adhesive strength measurements with wet tissue mimics

Lap shear adhesion experiments were performed using modified ASTM standard F2255-05. Collagen film were hydrated by immersing in 1X PBS for 15 minutes. Collagen/cellulose films[26] and polyethylene terephthalate squares of 20 × 20 × 0.02 mm were fixed onto slides using double-sided

tape. Bioadhesive (~20 mg) was pipetted onto the PET and the sample slides were clipped by applying 27 ± 5 kPa pressure with paper clips and photocured with an effective UVA dose (365 nm) of 20 J cm^{-2}. Shear adhesive strength failure was performed with a tensile tester (Chatillon Force Measurement Products, USA) at strain rate of 3 mm min^{-1} with 50 N loading cell.

2.5 Swelling Ratios of photocured bioadhesives

To study the swelling behaviour of cured bioadhesive formulation nearly 4-6 mg of uncured samples was pipetted onto 10 mm^2 PET sheets and cured. The samples where then immersed in 1X PBS at 37ºC for 1 hour. Samples were taken out of the buffer and their weight measured after cleaning their surface with lint-free papers. The percent swelling was calculated using the following equation

$$\%Swelling = \frac{W_b - W_o}{W_o} * 100 \quad (1)$$

where W_h is the weight of the hydrated sample and W_0 is the initial dry weight of the sample.

2.6 Exposure to platelet rich plasma and platelet adsorption/activation

Cured samples were rehydrated in 2 mL of 1X PBS for 2 hrs, then transferred to a sterile 24 well plate and blotted with lint free tissues (Kimwipes) to remove excess PBS. Blood from healthy human volunteers (ethics approval NTU-IRB reference number: IRB-2015-07-214) was mixed with 3.8 wt% of sodium citrate solution at a 9:1 v/v dilution ratio (blood/citrate) upon draw. Citrated blood was then centrifuged at 95×g at 8 °C for 15 mins. The transparent layer was pipetted to another vial and diluted 1:1 v:v with 1X PBS to obtain the platelet-rich plasma (PRP). PRP (75 uL) was dispensed onto cured samples (1 cm^2) placed in a 24 well microplate and incubated at 37°C for 1 hour in a 5% CO_2 cell culture incubator. After incubation, the samples were gently rinsed three times with 1X PBS. The adherent platelets were fixed with 3 vol % glutaraldehyde (in PBS) overnight at 4 °C. After fixation, the samples were thrice rinsed with 1X PBS followed by serial dehydrated by incubating in 10%, 25%, 50%, 75%, 90%, and 100% ethanol for 10 mins each. To quantify platelet adhesion and activation, dried sampled were coated with platinum for 40 seconds (JEOL Japan sputter coat) and

imaged using scanning electron microscopy (SEM) observation. The results were interpreted qualitatively (qualitative observation of SEM photomicrographs) and quantitatively (calculating the average number of adhered and activated platelets/mm^2 of the surface and the percentage of activated platelets to the total number of adhered platelets). Three representative SEM images were averaged at a resolution of 2000X (750 μm^2) and normalized to 1 mm^2. Platelets were defined in terms of morphology; resting stage platelets (non-dendritic, round profile) or activated platelets. Activated platelets were subjectively categorized as early stage activation (short-dendritic cells, pseudopods less than cell diameter or elongated platelets) and platelets at subsequent stage of activation (long-dendritic, pseudopods greater than cell diameter) [3].

2.7 Statistical analysis

Samples for rheometer, lap shear adhesion and swelling were performed in triplicate. The quantitative results were expressed as the mean ± standard deviation (SD) for n=3. The data were statistically analyzed using an analysis of variance at a significance level of $*p < 0.05$.

3. Results

3.1 PAMAM-g-diazirine bioadhesive composites are synthesized to challenge cationic charge, metabolic initiative, and stealth effects

Five formulations of PAMAM-g-diazirine bioadhesive are prepared to investigate the structure activity relationships in regards to human platelet adsorption and subsequent activation. An ideal implanted substrate would mimic the intima endothelial cell layer within veins and arteries—under normal, homeostasis conditions, platelets do not absorb or activate on the intima surface. This is the long-term goal of specific blood-contacting synthetic materials e.g. soft tissue fixatives. PAMAM dendrimers (from 4^{th} to 6^{th} generation) adhere and activate platelets because of their net positive charge offered by their terminal amine groups. PAMAM with anionic and neutral surface charges has shown to have platelet resistant properties and have shown minimal platelet adhesion [25]. **Fig. 1**

outlines the preparation of the formulations **III** to **VII**. A one-step synthesis grafts bromo-diazirine **II** onto G5-PAMAM **I** which has 128 surface 1° amines available. Rotary evaporation followed by drying under high vacuum removes solvent and HBr to yield the bioadhesives **III** and **IV**. At 15 and 30% diazirine grafting, the G5-PAMAM dendrimers are miscible in PBS buffer, but it should be noted that the phosphate buffer will be overwhelmed by the basicity of PAMAM free amines. From **III**, formulations **V**, **VI**, and **VII** are prepared to compare the reduction of cationic charge, metabolic initiative, or stealth effect approach, respectively. The cured samples are dehydrated and stored dry and then rehydrated in PBS when human blood donors are available. PBS rehydration serves to equilibrate the crosslinked films to physiological pH and remove any traces of HBr that may remain from the synthesis. The cured samples are then incubated in platelet rich plasma (PRP) and further processed for surface analysis by SEM.

Figure 1. a) Synthesis of PAMAM-g-diazirine (**III & IV**) and amine-capped PAMAM-g-diazirine (**V**) via chemical functionalization of terminal amines. **VI** and **VII** were physically mixed and photocured to obtained the crosslinked composite.

3.2 Carbene bioadhesive composites transition into viscoelastic solids with <10 J.cm^{-2} UVA light but amine-capped (V) PAMAM remains a viscoelastic liquid

The photorheometer analysis of the bioadhesive formulations **III-VII** determines the dynamic mechanical properties of storage modulus (G') and loss modulus (G") in real-time. This allows correlation of the UVA light dose to the mechanical properties as carbene mediate crosslinking proceeds only under irradiation[27]. Before irradiation the samples are subjected to 1s^{-1} oscillatory shear rate, where disruption of non-specific bonds (such as hydrogen bonding) decrease the storage modulus (G') for **III**, **IV,** and **V**, as seen in the first 30 s of **Fig. 2a**. The dynamic viscosity (G"/ang. freq.) of the uncured formulation is effected by the type of additive being used with **V** showing the lowest loss modulus (G") due to the loss of electrostatic amines into acetyl groups, as shown in **Table 1** and **Fig. 2a**. Doubling the diazirine grafting increases the probability of carbene-crosslinking,

leading to higher G' when photocured, but has an order of magnitude higher dynamic viscosity at the onset of **IV** in comparison to **III**. The high molar mass of alginate (> 300 kDa) in **VII** increases the G" by an order of magnitude when compared with **III**, likely due to chain entanglement and electrostatic interactions.

All formulations in **Fig. 2a** are observed to have G">G', viscoelastic liquids. Upon UVA irradiation, G' increases faster than G" due to carbene crosslinking .All formulation except **V** reached gelation (G"=G') between 40 – 50 s and continue to crosslink. The amine-capped formulation **V** had the lowest observed storage and loss modulus. After exposure to 20 J cm^{-2} UVA light, formulation **IV** showed the highest G' (78 ± 11 kPa). Addition of 15% heparin (25 ± 8 kPa) in **VI** and 3% Alginate (29 ± 3 kPa) in **VII** improved the storage modulus when compared to **III** (16 ± 4 kPa).

The elastic behaviour of the cured formulation were compared with an amplitude sweep after exposure to 20 J cm^{-2} irradiation. As seen in **Fig. 2b**, the stress-strain profile of the cured formulation mimics the J-curve response of soft tissues[28]. Like tissue deformation of blood vessels[29]; cured adhesives undergo large deformation at low stress (mimicking elastin dominated deformation) followed by strain hardening (mimicking collagen dominated deformation) at higher stresses. Formulation **IV**, is stiffest owing to higher diazirine grafting. All cured formulations have a yield range between 80-90% shear strain, but no linear viscoelastic ranges is observed. Formulation **V** does not observe any notable elastic behaviour at the shear rate applied.

Figure 2: A,B) Curing kinetics and stress-strain curve of formulation, **III IV V VI.15** and **VII** when cured with 365 nm UV with effective dose of 20 J cm^{-2}. C) Lap shear bioadhesion strength of the formulation when cured with 365 nm UV with effective dose of 20 J cm^{-2} against hydrated collagen films. D) Swelling behaviour (1hour) of cured formulations upon incubating it in 1X PBS at 37^{o}C.

3.3 Composites retain ability to bond wet substrates

Lap shear adhesion is assessed with a modified ASTM F 2255-05 protocol with substrates of hydrated collagen/cellulose films whose material properties mimic soft tissues[26] . The failure load from the load-displacement curve is used to calculate the maximum adhesion strength of the cured adhesives. in the results are summarized in **Fig. 2c**, where the lap shear strength of the formulations ranges between 8 – 45 kPa. Formulation **III, VI.H15** and **VII** display consistent adhesion strength between 8-10 kPa while formulation III shows five-fold improvement. These can be attributed to two reason; higher degree of diazirine grafting upon photocuring leads to a higher covalent attachment surface density of the collagen/cellulose film . , the bioadhesion strength for **V** is three times higher than **III**, and this is attributed to the viscoelastic dissipation as seen in water-based pressure sensitive adhesives[30]. The swelling behaviour of the cured bioadhesives gives an indication of the chemical crosslinking and solvent accessibility{Holback, 2011 #. Cured adhesives are immersed in PBS at 37°C for 1 hour and their swelling ratio recorded, as summarized in **Fig. 2d**. **V** swelled and disintgrated within the PBS, suggesting limited to no intermolecular crosslinking between the dendrimers. III, VI, and VII swelled between 200 - 250% within 1 hr, suggesting similar densities in intermolecular crosslinking and accessible water porosity.

3.4 Diazirine grafting has a significant reduction in platelet adhesion, but no effect on platelet activation.

The platelet response from PAMAM-g-diazirine **III** and **IV** are evaluated with PRP donated from healthy human volunteers. **Fig. 3** displays representative SEM photomicrographs of adhered platelets over the surfaces of PLGA (as control) and bioadhesives of **III** and **IV**. A positive control of 0% grafted **I** is not possible due to PAMAM's aqueous solubility within the PRP—it cannot be UV cured without diazirine grafting.

Figure 3. SEM photomicrographs of adhered and activated platelets on PLGA (**a, e**), **III** (**b, f**), **IV** (**c, g**), and **V** (**d, h**) at magnifications of 2000X (**a, b, c, d**) and 10,000X (**e, f, g, h**). **Green arrows**: senescent round platelets (non-dendritic), **blue arrows**: early stage activation (short dendritic) and **red arrows**:

late stage activation (long dendritic); **i, j** Quantitation of adhered and activated platelets on surfaces of **III, IV**, **V** and PLGA**.** Significant at * $p < 0.05$

Surface imaging of the fixed (via ethanol dehydration) and adhered platelets are identified by morphology; non-dendritic (**Fig. 3d,** green arrows), short dendritic (**Fig. 3e, 5g, & 5h**, blue arrows) and long dendritic (**Fig. 3f & 3g**, red arrows). Morphological changes are the most common criterion for qualitative assessment of platelet activation [3]. Inactivated platelets are characterized by their round morphology without having any spiny pseudopods (non-dendritic) and ascribed to resting stage platelets. Initial activation of platelets is identified by short pseudopods (short dendritic, short in relation to platelet diameter). Initial activation causes the platelets to become 'sticky' and change in shape to irregular spheres with multiple elongated pseudopodia (long dendritic) and signal advanced stages of platelet activation. Most of the platelets adhered to the bioadhesives **III** and **IV** were long dendritic in appearance irrespective of their diazirine conjugation percentage. Short dendritic platelets are observed in **IV** versus the entirety of the platelets observed on **III** are long dendritic in appearance. The results indicate that without further modification, **III** and **IV** have high thrombotic potential irrespective of diazirine conjugation percentage. **Fig. 3i** and **3j** summarizes the quantitative analysis of platelet adhesion and activation over the surfaces **III**, **IV**, and PLGA.

The quantitative results demonstrate that the number of adhered and activated platelets was reduced with an increase in diazirine concentration (**Fig. 3i**). There is no significant difference between degree of activation (activated platelets/total adhered platelets x 100) of substrates PLGA, **III** and **IV** (**Fig. 3j**). **IV** has a modest and significant improvement on platelet adherence, but both have several times the amount of platelets compared to control. The reduction/dilution in surface charge (due to pk_a shift from 1° to 2° amines, see supporting information) is speculated for the improvement seen in **IV**.

3.5 Acetylation of surface amines significantly decrease both platelet adhesion and activation.

To explore the contribution of surface charge towards platelet adhesion, the terminal amines of **III** are capped with acetyl chloride (**V**) to retain aqueous solubility and impart a neutrally charged dendrimer

surface. SEM photomicrographs of the platelets adhered to the bioadhesive surfaces of **III**, **V**, and PLGA are identified in **Fig. 3** and summarized in **Fig. 3i** and **3j**. SEM photomicrographs revealed the presence of non-dendritic and short dendritic platelets over the surface of cured **V**, visually indicating an inferior platelet activation compared to **III** and PLGA surfaces. The quantitative results in **Fig**. **5i** and **3.j** indicate both adhered and activated platelets were reduced with **V** and is in agreement with previously reported methods of reducing the platelet responses with amine modified PAMAM [25]. Capping of the amines to amides is hypothesized to create a neutral hydrophilic biomimetic surface with minimal thrombotic response, however this may not fully be the case. Amine quantification by the TNBS assay of uncured **III**, suggests that the majority of the amines are modified into amides or sterically inaccessible, as seen in **Fig. S1**. ^{1}H NMR results (see supporting information) suggest ca. 12% of the amines in **V** remain despite an 8x molar excess of acetyl chloride (73% acetylated + 15% diazirine grafting), supporting the likelihood of steric inaccessibility, a preselection of soluble polymer, or combination thereof.

3.6 Heparin composites of VI display inverse platelet adherence, but still have high levels of platelet activation.

Heparin, a well-known anticoagulant, is evaluated and compared at increasing wt% within the bioadhesive. Heparin is premixed with **III** at various ratios, and then photocured as normal to yield the composites **VI**. **Fig. 4a-h** displays the surface imaging of adhered platelets over the cured **VI (5-15%)** and cured **III** matrix washed with a solution of 5 wt% heparin.

Figure 4. SEM photomicrographs of adhered and activated platelets. Bioadhesive **III** are made into composites with 5 wt% of heparin (**VI.H5**; **a, e**), 10 wt% (**VI.H10; b, f**), and 15 wt% (**VI.H15; c, g**) and then photocured. Photocured **III** is washed with 5 wt% heparin (**III-H5**; **d, h**); Linear regression of activated platelets correlated to % heparin within **V**. **Green arrows**: senescent round platelets (non-dendritic), **blue arrows**: early stage activation (short dendritic) and **red arrows**: late stage activation (long dendritic); **i,j** Quantitation of platelet adhered and activation as a function of Heparin

concertation, heparin surface wash(III-H5) and PLGA. *Significant at $p < 0.05$, †: significantly different than all other formulations.

The activity of heparin is concentration dependent as adhered platelet density decreases as the heparin wt% increases in **VI**. Despite the decreasing platelet density, most of the platelets appear in the short or long dendritic stages. When **III** is washed with a pure solution of 5 wt% heparin, the lowest platelet density is seen compared with PLGA and **VI**, also a notable number of non-dendritic morphologies are present in the washed sample. The number of adhered and activated platelets was significantly reduced with higher ratios of heparin in **III**, compared to unmodified **III**. A minimum of 10% heparin in **VI** was required to have the comparable platelet response observed with PLGA control (there is no significant difference between **VI.H10** and PLGA, as seen in **Fig. 4i)**. Further increases in heparin ratio yields marginal improvements in preventing platelet adherence, but not in preventing platelet activation. The heparin wash is employed to mimic a high asymptote ratio of heparin in **III**. With the **III** surface blocked by heparin through electrostatic and covalent bonds (**Fig. 1b**), this approaches the limits of benign platelet response one can expect from synthetic surfaces. In this regard, the washed sample has a ca. 50% significant reduction in both adherence and platelet activation, as seen in **Fig. 4i**. **Fig. 4j** displays the strong inverse correlation of platelet adhesion density versus heparin concentration. Even though anti-fouling surfaces may not support significant platelet adhesion, they can still activate a limited number of platelets [31]. The results herein support the claim that heparin retains some therapeutic effects concerning anti-platelet adhesion whether it is incorporated in PAMAM bioadhesive composites or adsorbed onto the cured **III** surface, although long-term stability of heparin immobilization remains unresolved[32-33]. Heparin's anticoagulant ability appears to be negatively affected by the carbene crosslinking of **III** or the composite **VI** did not expose enough enough heparin to retain its natural ability despite loading up to 15%. In order to decrease the per cent of short and long dendritic platelets, other mechanisms need to be surveyed.

3.7 Bioadhesive composite VII offer the lowest % of activated platelets

PAMAM-g-diazirine **III** is mixed and cured with 3% sodium alginate (3% approaches the solubility limit) to prepare the composite **VII**. The antiplatelet ability of **VII** is evaluated as above and compared with **III** (no additive control) and PLGA. **Fig. 5a** and **b** shows the surface imaging and the averaged counts.

Figure 5. SEM photomicrographs of adhered and activated platelets over the bioadhesive surface of **VII** at magnification of 2000X (**a**) and 5,000X (**b**); Comparative quantitation of adhered and activated platelets (**c**), activated/adhered ratio **(d**) over the bioadhesive surfaces of **III**, **VII**, and PLGA (NS, No significant difference). **Green arrows**: senescent round platelets (non-dendritic), **blue arrows**: early stage activation (short dendritic) and **red arrows**: late stage activation (long dendritic); *Significant at $p < 0.05$, †: significantly different from **III** and PLGA.

SEM images revealed that the cured **VII** matrix is relatively smooth surface compared to PLGA (**Fig. 3a**) or **V** (**Fig. 4a-g**) formulations and has a better platelet anti-adhesion (adhesion) than PLGA or **III** controls. Surface imaging displays resting stage platelets on **VII** with little to no short/long dendritic cells as seen in **Fig. 5a**. To error on the side of caution, elongated platelets with no pseudopods are classified as short dendritic as seen in **Fig 5b** (blue arrows). No significant difference is observed between **VII** and PLGA, as seen in **Fig. 5c** and **5d** . However, platelet activation is reduced to 12% in **VII** compared to ca. 99% in **III** or PLGA. The results indicate that the alginate composite bioadhesive **VII** may be applicable where antifouling platelet surfaces are sought, but this requires follow-up investigation to gauge its long term fouling properties and local tissue histocompatibility studies, which are objectives of our future work.

4. DISCUSSION

Carbene-mediated bioadhesives offer a new mechanism to bond wet tissue substrates, with on-demand activation by photocuring [22-23, 27, 34]. Beyond sutures, few options are available for mending blood-contacting soft tissues - this creates a current unmet clinical need for rapid anastomosis techniques [35-37]. To evaluate carbene-mediated bioadhesive's potential for fixation of blood contacting soft tissues, PAMAM dendrimers are grafted with the carbene precursor, bromo-diazirine and a subsequent appraisal of the thrombotic potential is undertaken in this work with the aid of platelet rich plasma (PRP) from human blood samples. To our knowledge, there is no clinical bioadhesive that allows fixation of soft, blood contacting tissues that prevents platelet activation. Photo-activated carbene crosslinking (ability imparted by diazirine grafting) has the advantage of curing within seconds to minutes—a clear advantage over two-part bioadhesives that requires complete mixing before application. Possible clinical applications include blood vessel anastomoses, repair of aneurysms, and fixation of biosensors to arteries. However, even if the bioadhesive can bond to these wet substrates, in needs to be evaluated in terms of blood compatability. PRP exposure offers a rapid method for biomaterials evaluation of blood compatibility and artificial medical implants although many other methods exist depending on the hematology parameters sought [38-39]. As per ISO 10993-4, established whole blood and PRP exposure assays are recommended [40]. Platelets within plasma can be considered sensitive sensors whose morphology gives an indication of thrombosis risk. The activation is easily assessed from their rounded (senescent) to dendritic appearance (activated platelets) with high resolution surface imaging, attained by SEM imaging. Human derived PRP exposure allows for a rapid method of thrombotic risk assessment in terms of surfaces that may be exposed to blood in low shear conditions. Whole blood exposure assay requires the evaluation of complex blood parameters including counts of several cell types (flow cytometry and expensive markers), plasma haemoglobin (protein and ELISA assays), coagulation profile (temporal associations), and platelet function (biochemical assays) [41-42]. As these blood parameters change unpredictably in human donors and the assays themselves become cumbersome, the human PRP assay was preferred to simplify and rapidly assess the bioadhesive surfaces without sacrificing

human associated responses and risk factors. We recognize that this relatively simple assessment doesn't replace whole blood protocols, however it does allow a cost effective and rapid comparative evaluation among the bioadhesive formulations at blood/material interfaces. Secondly, the platelet adhesion and activation can be influenced by the elasticity of the cured formulation while their ability to adhere on the soft tissue dictates their patency with regard to interfacial failure under physiological stress. In this regard, three strategies were challenged against human derived PRP incubation: 1) reducing the concentration of cationic surface amines (**III**, **IV**, & **V**), 2) incorporating anti-coagulant/antifouling additives (**VI** and **VII**), and 3) surface coverage of the cured cationic bioadhesive with the anticoagulant 25 kDa heparin (**III** + heparin wash). Based on the platelet studies, the formulation were further characterized for their mechanical properties, wet tissue adhesion strength, and swelling ratios. For formulation **VI**, only 15% Heparin additive was characterized as it showed the lowest platelet adhesion and activation.

As expected, when cationic charges were sterically shielded with additional diazirine grafting, (**III** → **IV**, 1° to 2° NH_2) a ca. 20% drop in platelet adherence was seen, but with no significant difference in % platelet activation, nearly all adhered platelets were activated (**Fig. 5**). Converting the majority of 1° amines to neutral amides (**III** → **V**) reduced platelet adherence 3-fold, similar to PLGA control with a significant reduction of platelet activation (vs. PLGA, **III**, or **IV**). Both **III** and **IV** forms a covalently crosslinked networked but doubling the diazirine grafting in **IV** resulted in a cured storage modulus 5x higher than **III**, with similar elongation (Fig 2a & 2b). The mechanical properties and swelling disintegration of the amine-capped **V** suggests that intermolecular crosslinking may have some dependence on photoinduced diazo formation that forms covalent crosslinks with nucleophiles (e.g. amines, carboxylic acids). Aryl diazirines have been observed to isomerize into diazo compounds and subsequently react with nucleophiles{Smith, 1975 #112}. Despite limited intermolecular crosslinking, **V** had lap shear adhesion 3x **III**, which is likely due to viscoelastic dissipation, similar to the mechanisms incorporated within pressure sensitive adhesive tapes. Despite the additional diazirine grafting of **IV** and amine-capping of **V**, the majority of the platelets (>80%) were exhibiting short/long dendritic phases and thus considered at high risk for inducing thrombosis.

Recent reports have attributed the thrombosis potential of PAMAM dendrimers (in solution, not as hydrogel surfaces) solely to the cationic surface charge[25, 43-44]. Others have observed that key modifications of PAMAM induce it to be a potential antithrombotic therapy[45]. However, under the scope of crosslinked tissue adhesive, the high % of platelet activation in formulations **III**, **IV**, and **V** suggest more factors may be responsible. Regardless, another strategy is required to lower the risk of platelet adhesion and activation on PAMAM bioadhesive surfaces.

The unique on-demand cross-linking of PAMAM-g-diazirine dendrimer was exploited towards the synthesis of hydrophilic composites incorporating polysaccharides (heparin and alginate) known to have antifouling properties. To our knowledge, **VI** 5-15% heparin ratios are the first reported composites of PAMAM and heparin applied towards antiplatelet surfaces, although PAMAM/heparin constructs have been synthesized for controlled release purposes [46-47]. The immobilization of anticoagulant has shown to enhance the blood compatibility of polymer based hydrogels, but can ultimately reduce the activity versus free heparin. [14 48]. Cationic dendrimers strongly interact with anionic heparin via electrostatic interactions, which is often exploited for non-viral gene delivery where optimization is required to maximize cell uptake (endocytosis), but minimize cationic toxicity[47, 49-50 51 52]. The doses of heparin had a strong correlation on platelet adherence as seen in **Fig. 3j**, but no correlation on platelet activation (>95% activation for all **VI**). At high enough ratios, **VI.H15** displayed half the platelet adhesion of PLGA control, but **VI** is unlikely to be further optimized with larger ratios of heparin. The dose dependant reduction of platelet adhesion could be due to the shielding effect of anions (in heparin) to the cationic amine groups in PAMAM-g-diazirine. The composite bioadhesive formulations were prepared with gradual decrease in the ratio of +/- charge (amines in PAMAM-g-diazirine/ sulphate + carboxylate groups in heparin, see supporting information). The results demonstrated the significant reduction in platelet adhesion as the +/- ratio dropped from **11 to 3.7** (see **Table S2**) and was in agreement with our hypothesis, even though other cationic polymer/heparin composites are known to inactivate heparin[53].

The cationic surface charge and labile diazo groups of light-cured **III** was exploited to electrostatically coat heparin on the surface in **III-H5**, but covalent bonds may form as well. A

fraction of the light activated carbenes isomerize to diazo groups upon photoactivation, raising the possibility of covalent crosslinking of heparin to PAMAM[54]. Regardless, the heparinized surface displayed the lowest platelet adherence of all formulations evaluated, with 46% of the platelets in a non-dendritic, senescent state.

Several polysaccharides such as chitosan, dextran, alginate, and hyaluronic acid are used as the backbone of hydrogels to improve the mechanical properties of hydrogel formulations [55]. Among these polysaccharides, alginate hydrogels are promising as antifouling/antithrombotic additives in various biomedical applications[19, 56-57]. Alginate is a linear copolymer of >350 kDa that is easily crosslinked by chelating cations (e.g. Ca^{2+}, Ba^{2+}, and Mg^{2+}) and forms hydrogels with a molar mass as low 40 kDa [58]. Aiming to prepare an antifouling PAMAM-g-diazirine hydrogel with respect to platelets, composite formulation comprising **VII** was synthesized with 3% alginate, which approaches alginates solubility limit [59 60 61]. This formulation had the lowest platelet activation of all formulations assessed, with more than 88% platelets displaying non-dendritic morphologies or a activated platelet density of 300 platelets mm^{-2}. The antiplatelet properties of the alginate modified formulation may be due to stealth effects, which is often ascribed to PEG coatings[62]. The stealth effect is speculated to limit or prevent adsorption of albumen, fibrinogen, or other proteins that correlate with platelet activation [57, 63]. Considering that both composites retained lap shear adhesion to wet substrates similar to **III** with a significant improvement in non-activation of human derived platelets, these composites will be chosen towards in vivo assessment in our future work. The lap shear adhesive strengths ranged from 8 - 46 kPa for all fomulations, compared to 1-3 kPa for fibrin sealants[9]. Alginate bioadhesives composites were observed to have the most optimized material properties in regards to platelet inactivation, adhesion, and modulus (results herein), but potential drawbacks are noted. Alginates propensity to chelate or exchange Ca^{2+} and other cations in physiological mediums will change the mechanical properties over time (unpredictable shifts in modulus and integrity) and may limit long-term stability [64-65]. However, the results presented herein with carbene covalent crosslinking may mediate these effects[60].

4. Conclusion

Herein, the risk evaluation of thrombogenic responses was performed with a platelet rich plasma from human donors on PAMAM-g-diazirine photocured bioadhesives and associated composites. Reduction of cationic charge by additional diazirine grafting or acetylation of surface amines reduced platelet adherence to that of PLGA control (in the case of acetylation), but had little to no effect on platelet activation, but there was significant shifts in intermolecular crosslinking, lap shear adhesion, and swelling. For the first time, heparin and alginate composites were easily produced with carbene precursor adhesives in a one-step, light activated reaction. Composites were quantitatively assessed for platelet adherence and activation through SEM surface imaging. Heparin composites displayed an inverse linear correlation (R^2 = 0.90) of platelet adherence vs heparin concentration, from 5 - 15% heparin addition. Cured bioadhesive (with no additives) rinsed with heparin solution had the lowest amount of platelet adhesion with 46% of the platelets in a senescent, non-activated state. Alginate composites had the lowest surface density of activated platelets at 300 platelets mm^{-2}, a 97% reduction compared to PAMAM-g-diazirine (15%) cured films. Despite the addition of heparin and alginate additives, mechanical properties, adhesion strength, and swelling ratios of PAMAM-g-diazirine (15%) bioadhesive is retained.

Acknowledgements

Authors acknowledge support from the following research grants: Ministry of Education Tier 1 Grant (RG47/16): Coil Expanding Layers (COELS) For Intravascular Repairs, Ministry of Education Tier 2 Grants: 1) Tailored soft-tissue bioadhesives for site-specific therapy (MOE2012-T2-2-046) and 2) Reversible, electrocuring adhesives (MOE2014-T2-2-100); NTU-Northwestern Institute for Nanomedicine Grant: 3D-Printing of Electro-Curing Nanocomposite Living Electrodes for Cardiac Tissue Regeneration.

Supporting information: Diazirine grafting analysis, NMR spectra, degree of acetylation, and charge ratio: PAMAM-$amino^+$ / (SO_3^- + COO^-)-heparin calculations.

References.

1. Aguilar, M. R.; Rodríguez, G.; Fernández, M.; Gallardo, A.; San Román, J., Polymeric active coatings with functionality in vascular applications. *J. Mater. Sci. Mater. Med.* **2002,** *13* (12), 1099-1104.
2. Rodrigues, S. N.; Gonçalves, I. C.; Martins, M.; Barbosa, M. A.; Ratner, B. D., Fibrinogen adsorption, platelet adhesion and activation on mixed hydroxyl-/methyl-terminated self-assembled monolayers. *Biomaterials* **2006,** *27* (31), 5357-5367.
3. Goodman, S. L., Sheep, pig, and human platelet-material interactions with model cardiovascular biomaterials. *Journal of biomedical materials research* **1999,** *45* (3), 240-250.
4. Kamath, S.; Blann, A.; Lip, G., Platelet activation: assessment and quantification. *European heart journal* **2001,** *22* (17), 1561-1571.
5. Jennings, L. K., Mechanisms of platelet activation: need for new strategies to protect against platelet-mediated atherothrombosis. *Thromb Haemost* **2009,** *102* (2), 248-257.
6. Zhao, J. Z., Coating Employing an Anti-Thrombotic Conjugate. Google Patents: 2007.
7. Ragheb, A. O.; Bates, B. L.; Boatman, S. E.; Burton, D. G.; Hoffa, M. C.; Schaeffer, D. G.; Sturgeon, J. S., Coated medical device. Google Patents: 2010.
8. Spotnitz, W. D., Fibrin Sealant: The Only Approved Hemostat, Sealant, and Adhesive—a Laboratory and Clinical Perspective. *ISRN Surgery* **2014,** *2014*, 28.
9. McDermott, M. K.; Chen, T.; Williams, C. M.; Markley, K. M.; Payne, G. F., Mechanical Properties of Biomimetic Tissue Adhesive Based on the Microbial Transglutaminase-Catalyzed Crosslinking of Gelatin. *Biomacromolecules* **2004,** *5* (4), 1270-1279.
10. Liu, C. D.; Glantz, G. J.; Livingston, E. H., Fibrin glue as a sealant for high-risk anastomosis in surgery for morbid obesity. *Obesity surgery* **2003,** *13* (1), 45.
11. Gibble, J.; Ness, P., Fibrin glue: the perfect operative sealant? *Transfusion* **1990,** *30* (8), 741-747.
12. Ferreira, P.; Silva, A. F. M.; Pinto, M. I.; Gil, M. H., Development of a biodegradable bioadhesive containing urethane groups. *J. Mater. Sci. Mater. Med.* **2008,** *19* (1), 111-120.
13. Queiroz, D. P.; Pinto, I. M.; Besteiro, M. C.; Silva, A. F.; Gil, M. H.; Guiomar, A. J.; de Pinho, M. N., Surface and hemocompatibility studies of bi-soft segment polyurethane membranes. *Int J Artif Organs* **2006,** *29* (9), 866-72.
14. Leszczak, V.; Smith, B. S.; Popat, K. C., Hemocompatibility of polymeric nanostructured surfaces. *Journal of Biomaterials Science, Polymer Edition* **2013,** *24* (13), 1529-1548.
15. Tang, L.; Thevenot, P.; Hu, W., Surface chemistry influences implant biocompatibility. *Curr. Top. Med. Chem.* **2008,** *8* (4), 270-280.
16. Biran, R.; Pond, D., Heparin coatings for improving blood compatibility of medical devices. *Adv. Drug Del. Rev.* **2017,** *112*, 12-23.
17. Yang, Z.; Wang, J.; Luo, R.; Maitz, M. F.; Jing, F.; Sun, H.; Huang, N., The covalent immobilization of heparin to pulsed-plasma polymeric allylamine films on 316L stainless steel and the resulting effects on hemocompatibility. *Biomaterials* **2010,** *31* (8), 2072-2083.
18. Hinrichs, W.; ten Hoopen, H. W.; Wissink, M.; Engbers, G.; Feijen, J., Design of a new type of coating for the controlled release of heparin. *J. Controlled Release* **1997,** *45* (2), 163-176.

19. Liu, M.; Yue, X.; Dai, Z.; Xing, L.; Ma, F.; Ren, N., Stabilized hemocompatible coating of nitinol devices based on photo-cross-linked alginate/heparin multilayer. *Langmuir* **2007,** *23* (18), 9378-9385.
20. Movsisyan, M.; Delbeke, E. I.; Berton, J. K.; Battilocchio, C.; Ley, S. V.; Stevens, C. V., Taming hazardous chemistry by continuous flow technology. *Chem. Soc. Rev.* **2016,** *45* (18), 4892-928.
21. Deadman, B. J.; Collins, S. G.; Maguire, A. R., Taming hazardous chemistry in flow: the continuous processing of diazo and diazonium compounds. *Chemistry* **2015,** *21* (6), 2298-308.
22. Feng, G.; Djordjevic, I.; Mogal, V.; O'Rorke, R.; Pokholenko, O.; Steele, T. W., Elastic Light Tunable Tissue Adhesive Dendrimers. *Macromol. Biosci.* **2016**.
23. Ping, J.; Gao, F.; Chen, J. L.; Webster, R. D.; Steele, T. W., Adhesive curing through low-voltage activation. *Nature communications* **2015,** *6*.
24. Nanda, H. S.; Singh, M.; Steele, T. W., Thrombogenic Responses from Electrocured Tissue Adhesives. *ECS Transactions* **2017,** *77* (11), 547-555.
25. Dobrovolskaia, M. A.; Patri, A. K.; Simak, J.; Hall, J. B.; Semberova, J.; De Paoli Lacerda, S. H.; McNeil, S. E., Nanoparticle size and surface charge determine effects of PAMAM dendrimers on human platelets in vitro. In *Mol. Pharm.*, 2011; Vol. 9, pp 382-393.
26. Steele, T. W.; Huang, C. L.; Nguyen, E.; Sarig, U.; Kumar, S.; Widjaja, E.; Loo, J. S.; Machluf, M.; Boey, F.; Vukadinovic, Z.; Hilfiker, A.; Venkatraman, S. S., Collagen-cellulose composite thin films that mimic soft-tissue and allow stem-cell orientation. *J Mater Sci Mater Med* **2013,** *24* (8), 2013-27.
27. Mogal, V.; Papper, V.; Chaurasia, A.; Feng, G.; Marks, R.; Steele, T., Novel on-demand bioadhesion to soft tissue in wet environments. *Macromol. Biosci.* **2014,** *14* (4), 478-84.
28. Lally, C.; Reid, A. J.; Prendergast, P. J., Elastic Behavior of Porcine Coronary Artery Tissue Under Uniaxial and Equibiaxial Tension. *Ann. Biomed. Eng.* **2004,** *32* (10), 1355-1364.
29. Zhou, J.; Fung, Y. C., The degree of nonlinearity and anisotropy of blood vessel elasticity. *Proceedings of the National Academy of Sciences* **1997,** *94* (26), 14255-14260.
30. Yang, H. W. H., Water-based polymers as pressure-sensitive adhesives—viscoelastic guidelines. *J. Appl. Polym. Sci.* **1995,** *55* (4), 645-652.
31. Hanson, S. R.; Harker, L. A.; Ratner, B. D.; Hoffman, A. S., In vivo evaluation of artificial surfaces with a nonhuman primate model of arterial thrombosis. *J Lab Clin Med* **1980,** *95* (2), 289-304.
32. Mao, C.; Qiu, Y.; Sang, H.; Mei, H.; Zhu, A.; Shen, J.; Lin, S., Various approaches to modify biomaterial surfaces for improving hemocompatibility. *Adv. Colloid Interface Sci.* **2004,** *110* (1), 5-17.
33. Park, K. D.; Okano, T.; Nojiri, C.; Kim, S. W., Heparin immobilization onto segmented polyurethaneurea surfaces—effect of hydrophilic spacers. *Journal of Biomedical Materials Research* **1988,** *22* (11), 977-992.
34. Gan, L.; Tan, N. C. S.; Steele, T. W. J., Incorporation of Conductive Internal Additives within Electrocuring Adhesives. *ECS Transactions* **2017,** *77* (11), 981-988.
35. O'Rorke, R. D.; Pokholenko, O.; Gao, F.; Cheng, T.; Shah, A.; Mogal, V.; Steele, T. W., Addressing Unmet Clinical Needs with UV Bioadhesives. *Biomacromolecules* **2017,** *18* (3), 674-682.
36. Vokrri, L.; Qavdarbasha, A.; Rudari, H.; Ahmetaj, H.; Manxhuka-Kerliu, S.; Hyseni, N.; Porcu, P.; Cinquin, P.; Sessa, C., Experimental study of sutureless vascular anastomosis with use of glued prosthesis in rabbits. *Vasc Health Risk Manag* **2015,** *11*, 211-7.

37. Kapischke, M.; Gerhard, D.; Pries, A., Sutureless open vascular anastomosis connector: An experimental study. *Vascular* **2017,** *25* (1), 101-104.
38. Zhou, L.; Tan, G.-X.; Ning, C.-Y., Modification of biomaterials surface by mimetic cell membrane to improve biocompatibility. *Frontiers of Materials Science* **2014,** *8* (4), 325-331.
39. Kim, Y. J.; Kang, I.-K.; Huh, M. W.; Yoon, S.-C., Surface characterization and in vitro blood compatibility of poly(ethylene terephthalate) immobilized with insulin and/or heparin using plasma glow discharge. *Biomaterials* **2000,** *21* (2), 121-130.
40. Seyfert, U. T.; Biehl, V.; Schenk, J., In vitro hemocompatibility testing of biomaterials according to the ISO 10993-4. *Biomol. Eng.* **2002,** *19* (2), 91-96.
41. Haycox, C. L.; Ratner, B. D., In vitro platelet interactions in whole human blood exposed to biomaterial surfaces: Insights on blood compatibility. *Journal of Biomedical Materials Research* **1993,** *27* (9), 1181-1193.
42. Sharma, C. P.; Hari, P. R., Surface modification of polystyrene--platelet adhesion. *J. Biomater. Appl.* **1990,** *5* (1), 49-55.
43. Jones, C. F.; Campbell, R. A.; Brooks, A. E.; Assemi, S.; Tadjiki, S.; Thiagarajan, G.; Mulcock, C.; Weyrich, A. S.; Brooks, B. D.; Ghandehari, H., Cationic PAMAM dendrimers aggressively initiate blood clot formation. *ACS nano* **2012,** *6* (11), 9900-9910.
44. Watala, C.; Karolczak, K.; Kassassir, H.; Siewiera, K.; Maczynska, K.; Pieniazek, A.; Labieniec-Watala, M., How do the full-generation poly(amido)amine (PAMAM) dendrimers activate blood platelets? Platelet membrane zeta potential and other membrane-associated phenomena. *Int. J. Pharm.* **2016,** *500* (1), 379-389.
45. Duran-Lara, E.; Guzman, L.; John, A.; Fuentes, E.; Alarcon, M.; Palomo, I.; Santos, L. S., PAMAM dendrimer derivatives as a potential drug for antithrombotic therapy. *Eur. J. Med. Chem.* **2013,** *69*, 601-8.
46. Bromfield, S. M.; Posocco, P.; Fermeglia, M.; Tolosa, J.; Herreros-Lopez, A.; Pricl, S.; Rodriguez-Lopez, J.; Smith, D. K., Shape-persistent and adaptive multivalency: rigid transgeden (TGD) and flexible PAMAM dendrimers for heparin binding. *Chemistry* **2014,** *20* (31), 9666-74.
47. Bai, S.; Ahsan, F., Synthesis and evaluation of pegylated dendrimeric nanocarrier for pulmonary delivery of low molecular weight heparin. *Pharm. Res.* **2009,** *26* (3), 539-48.
48. Beena, M.; Chandy, T.; Sharma, C. P., Heparin immobilized chitosan-poly ethylene glycol interpenetrating network: Antithrombogenicity. *Artificial Cells, Blood Substitutes, and Biotechnology* **1995,** *23* (2), 175-192.
49. Steele, T. W.; Shier, W. T., Dendrimeric alkylated polyethylenimine nano-carriers with acid-cleavable outer cationic shells mediate improved transfection efficiency without increasing toxicity. *Pharm. Res.* **2010,** *27* (4), 683-98.
50. Steele, T. W.; Zhao, X.; Tarcha, P.; Kissel, T., Factors influencing polycation/siRNA colloidal stability toward aerosol lung delivery. *European Journal of Pharmaceutics and Biopharmaceutics* **2012,** *80* (1), 14-24.
51. Klajnert, B.; Cangiotti, M.; Calici, S.; Ionov, M.; Majoral, J. P.; Caminade, A.-M.; Cladera, J.; Bryszewska, M.; Ottaviani, M. F., Interactions between dendrimers and heparin and their implications for the anti-prion activity of dendrimers. *New J. Chem.* **2009,** *33* (5), 1087-1093.
52. Bromfield, S. M.; Posocco, P.; Fermeglia, M.; Pricl, S.; Rodríguez-López, J.; Smith, D. K., A simple new competition assay for heparin binding in serum applied to multivalent PAMAM dendrimers. *Chem. Commun.* **2013,** *49* (42), 4830-4832.
53. Lorkowska-Zawicka, B.; Kaminski, K.; Ciejka, J.; Szczubialka, K.; Bialas, M.; Okon, K.; Adamek, D.; Nowakowska, M.; Jawien, J.; Olszanecki, R.; Korbut, R., Inactivation of heparin by cationically modified chitosan. *Mar Drugs* **2014,** *12* (7), 3953-69.

54. Brunner, J.; Senn, H.; Richards, F. M., "3-Trifluoromethyl-3-Phenyldiazirine - a New Carbene Generating Group for Photolabeling Reagents. *J. Biol. Chem.* **1980,** *255* (8), 3313-3318.
55. Hermanson, G. T., *Bioconjugate techniques*. Academic press: 2013.
56. Manabe, K.; Kyung, K. H.; Shiratori, S., Biocompatible slippery fluid-infused films composed of chitosan and alginate via layer-by-layer self-assembly and their antithrombogenicity. *ACS Appl Mater Interfaces* **2015,** *7* (8), 4763-71.
57. Zheng, J.; Xie, H.; Yu, W.; Tan, M.; Gong, F.; Liu, X.; Wang, F.; Lv, G.; Liu, W.; Zheng, G.; Yang, Y.; Xie, W.; Ma, X., Enhancement of surface graft density of MPEG on alginate/chitosan hydrogel microcapsules for protein repellency. *Langmuir* **2012,** *28* (37), 13261-73.
58. Ribeiro, C.; Barrias, C.; Barbosa, M., Calcium phosphate-alginate microspheres as enzyme delivery matrices. *Biomaterials* **2004,** *25* (18), 4363-4373.
59. Drury, J. L.; Mooney, D. J., Hydrogels for tissue engineering: scaffold design variables and applications. *Biomaterials* **2003,** *24* (24), 4337-4351.
60. Lee, K. Y.; Mooney, D. J., Alginate: Properties and biomedical applications. *Prog. Polym. Sci.* **2012,** *37* (1), 106-126.
61. Gomez, C.; Rinaudo, M.; Villar, M., Oxidation of sodium alginate and characterization of the oxidized derivatives. *Carbohydr. Polym.* **2007,** *67* (3), 296-304.
62. Schöttler, S.; Becker, G.; Winzen, S.; Steinbach, T.; Mohr, K.; Landfester, K.; Mailänder, V.; Wurm, F. R., Protein adsorption is required for stealth effect of poly(ethylene glycol)- and poly(phosphoester)-coated nanocarriers. *Nat Nano* **2016,** *11* (4), 372-377.
63. Fan, Y.; Luo, R.; Han, H.; Weng, Y.; Wang, H.; Li, J. a.; Yang, P.; Wang, Y.; Huang, N., Platelet Adhesion and Activation on Chiral Surfaces: The Influence of Protein Adsorption. *Langmuir* **2017,** *33* (39), 10402-10410.
64. Chou, A. I.; Akintoye, S. O.; Nicoll, S. B., Photo-crosslinked alginate hydrogels support enhanced matrix accumulation by nucleus pulposus cells in vivo. *Osteoarthritis and Cartilage 17* (10), 1377-1384.
65. Knight, M. M.; van de Breevaart Bravenboer, J.; Lee, D. A.; van Osch, G. J. V. M.; Weinans, H.; Bader, D. L., Cell and nucleus deformation in compressed chondrocyte–alginate constructs: temporal changes and calculation of cell modulus. *Biochimica et Biophysica Acta (BBA) - General Subjects* **2002,** *1570* (1), 1-8.

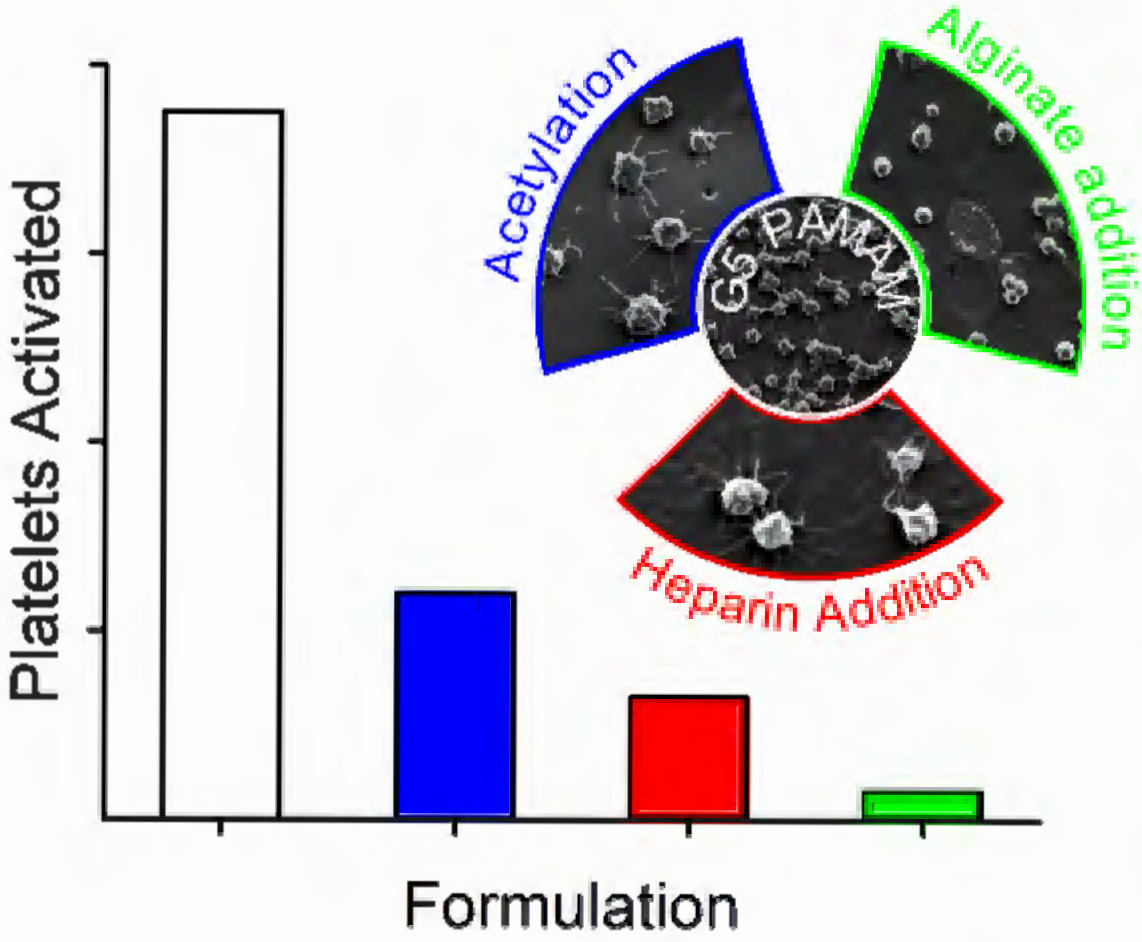
Platelets Activated
Formulation
Acetylation
Alginate addition
Heparin Addition
G5 PAMAM

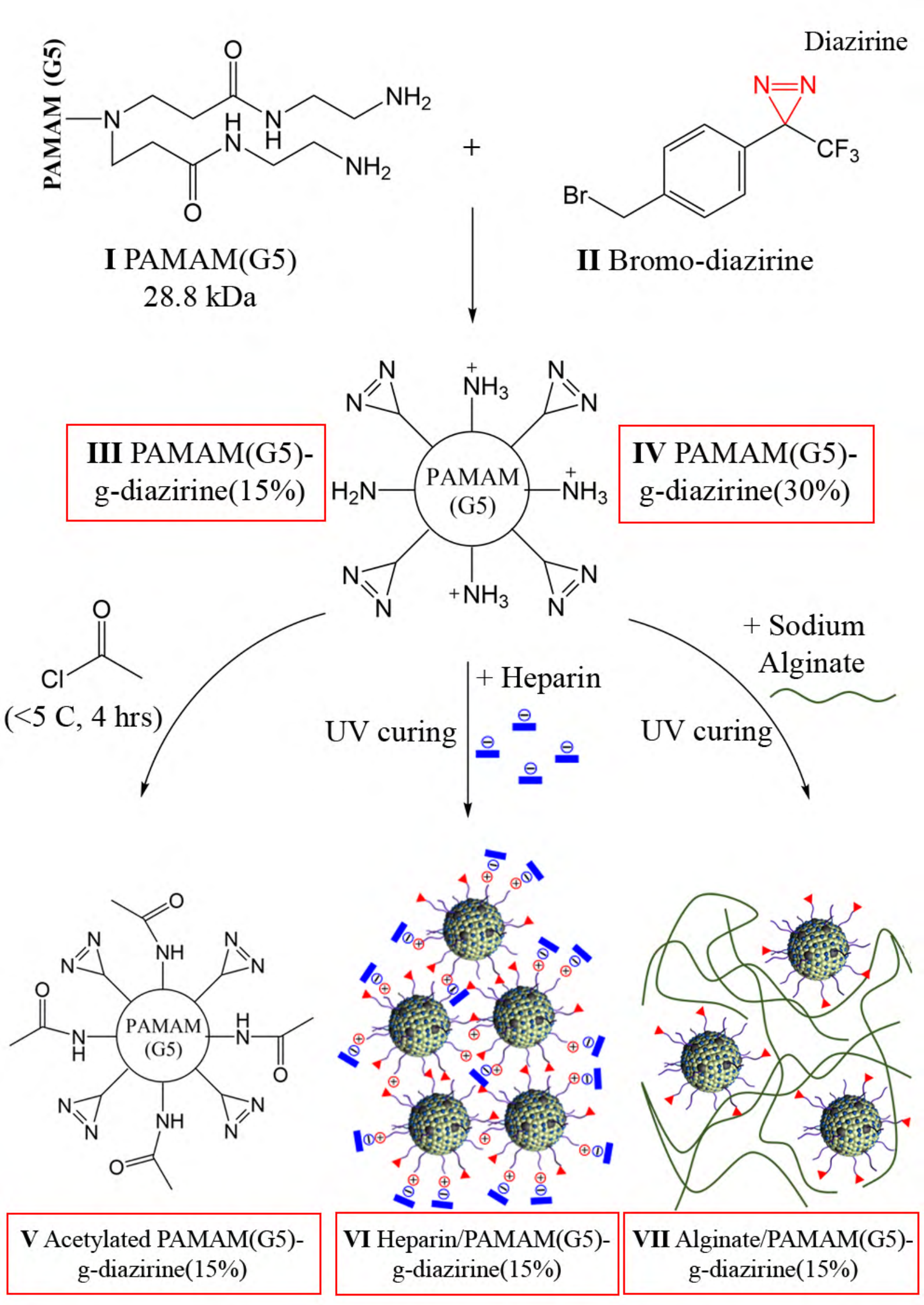
PAMAM (G5)
Diazirine
I PAMAM(G5)
28.8 kDa
II Bromo-diazirine
III PAMAM(G5)-g-diazirine(15%)
IV PAMAM(G5)-g-diazirine(30%)
PAMAM (G5)
(<5 C, 4 hrs)
+ Heparin
UV curing
+ Sodium Alginate
UV curing
V Acetylated PAMAM(G5)-g-diazirine(15%)
VI Heparin/PAMAM(G5)-g-diazirine(15%)
VII Alginate/PAMAM(G5)-g-diazirine(15%)

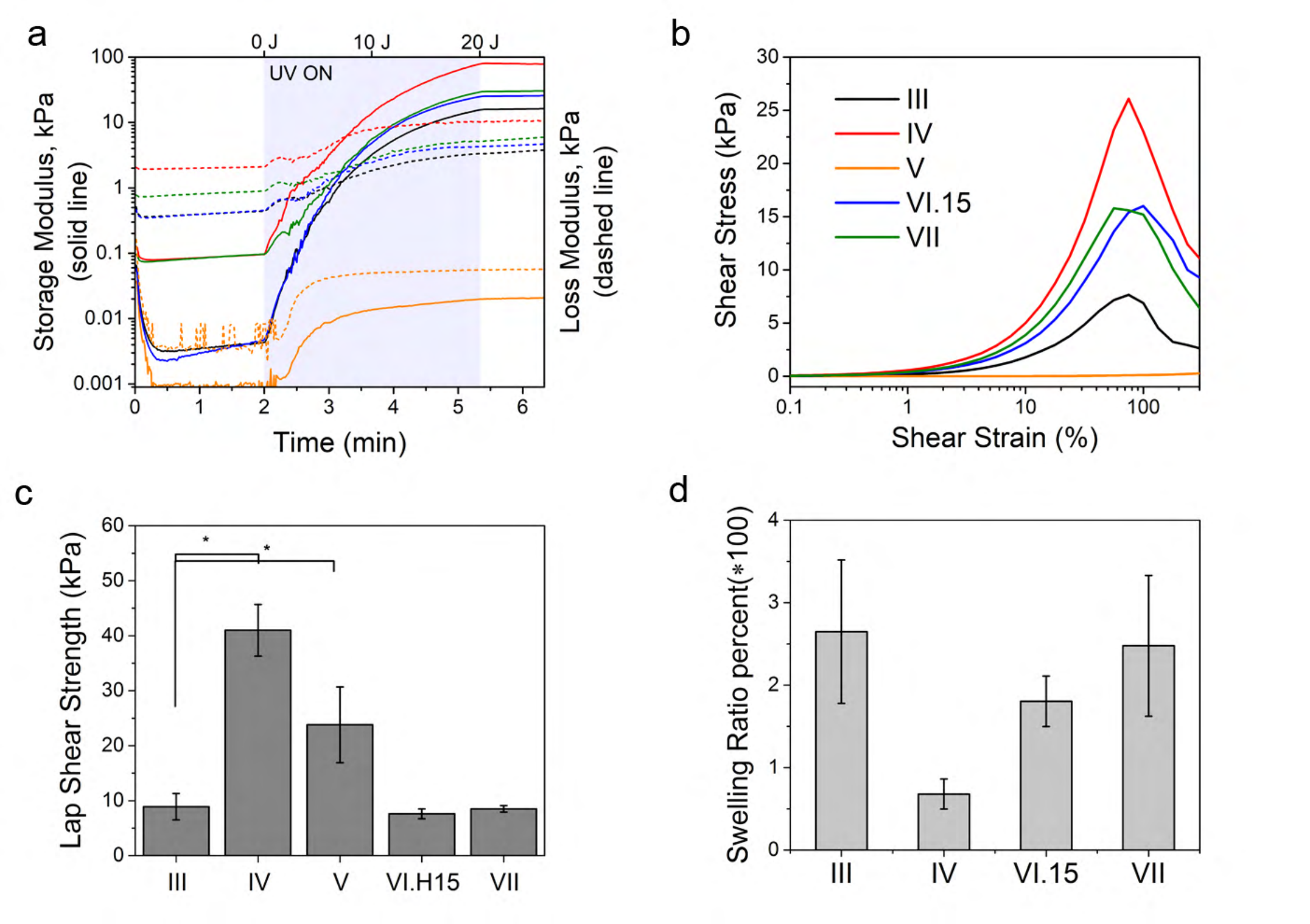
a
0 J
10 J
20 J
UV ON
Storage Modulus, kPa
(solid line)
Loss Modulus, kPa
(dashed line)
Time (min)
b
III
IV
V
VI.15
VII
Shear Stress (kPa)
Shear Strain (%)
c
Lap Shear Strength (kPa)
III
IV
V
VI.H15
VII
d
Swelling Ratio percent(*100)
III
IV
VI.15
VII

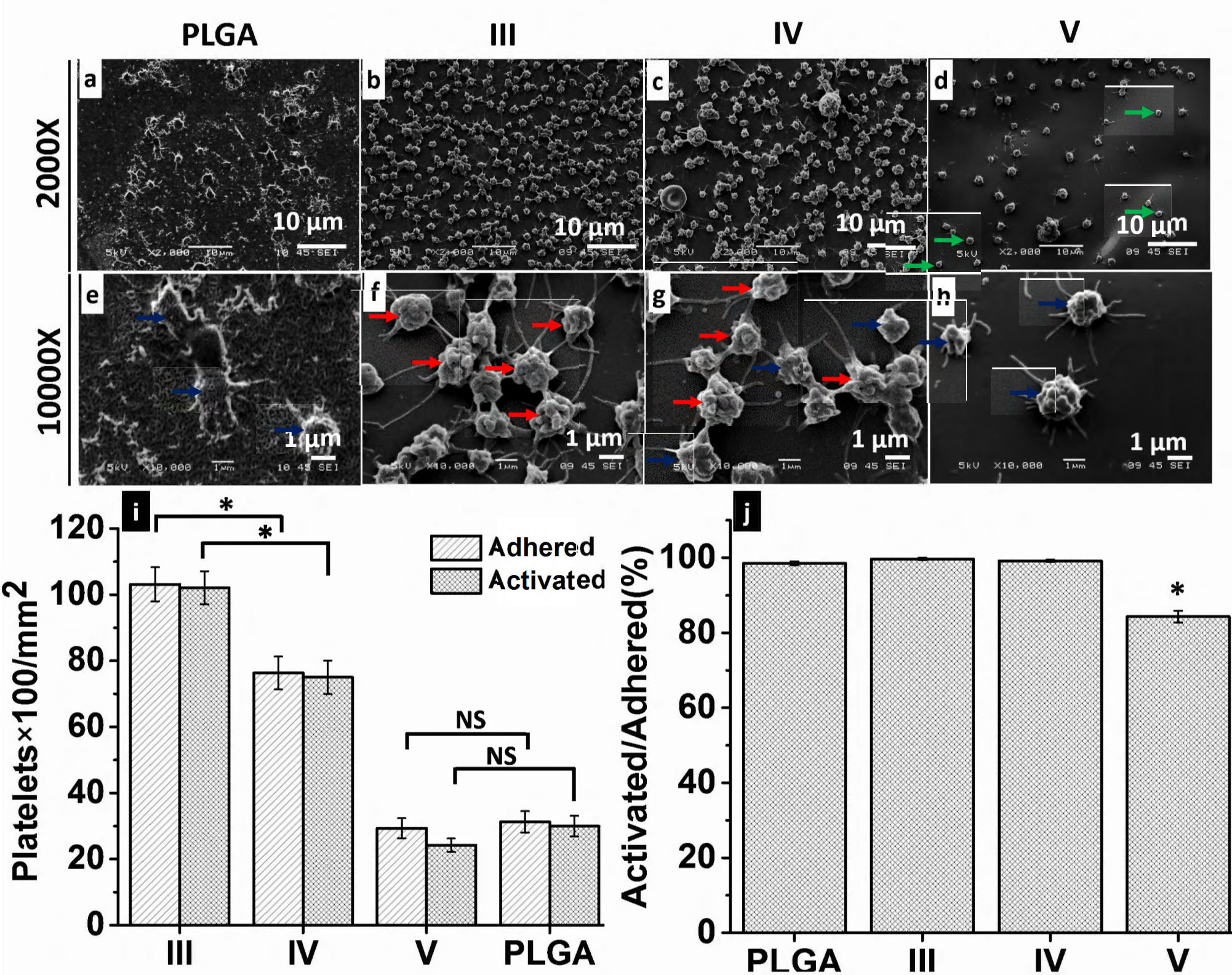
PLGA
III
IV
V
2000X
10000X
a
b
c
d
e
f
g
h
10 µm
1 µm
i
j
Adhered
Activated
Platelets×100/mm2
Activated/Adhered(%)
NS
*
III
IV
V
PLGA

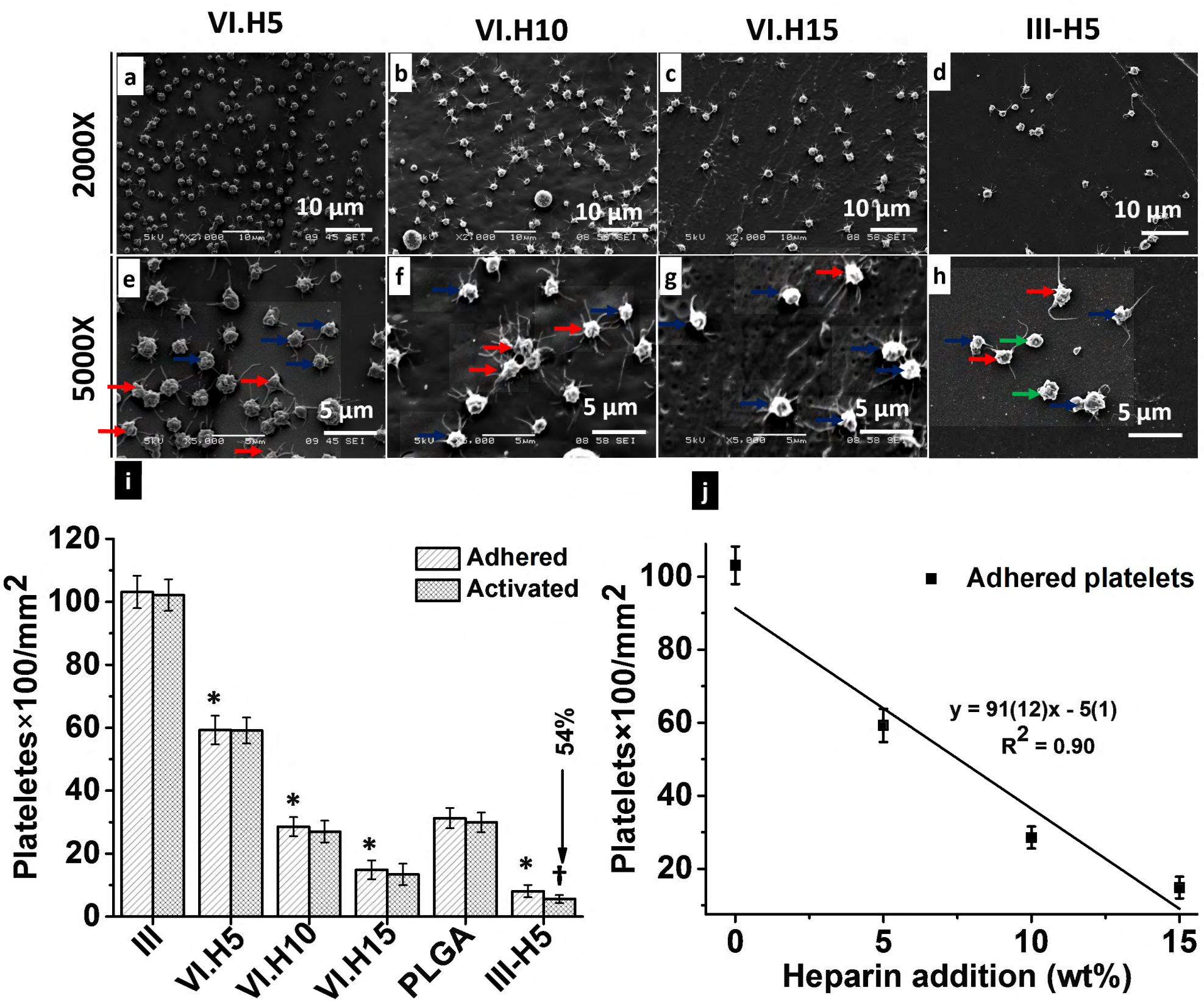
VI.H5
VI.H10
VI.H15
III-H5
2000X
5000X
a
b
c
d
e
f
g
h
10 µm
5 µm
i
j
Adhered
Activated
Platelets×100/mm2
120
100
80
60
40
20
0
*
54%
III
VI.H5
VI.H10
VI.H15
PLGA
III-H5
Adhered platelets
y = 91(12)x - 5(1)
R2 = 0.90
Heparin addition (wt%)
0
5
10
15

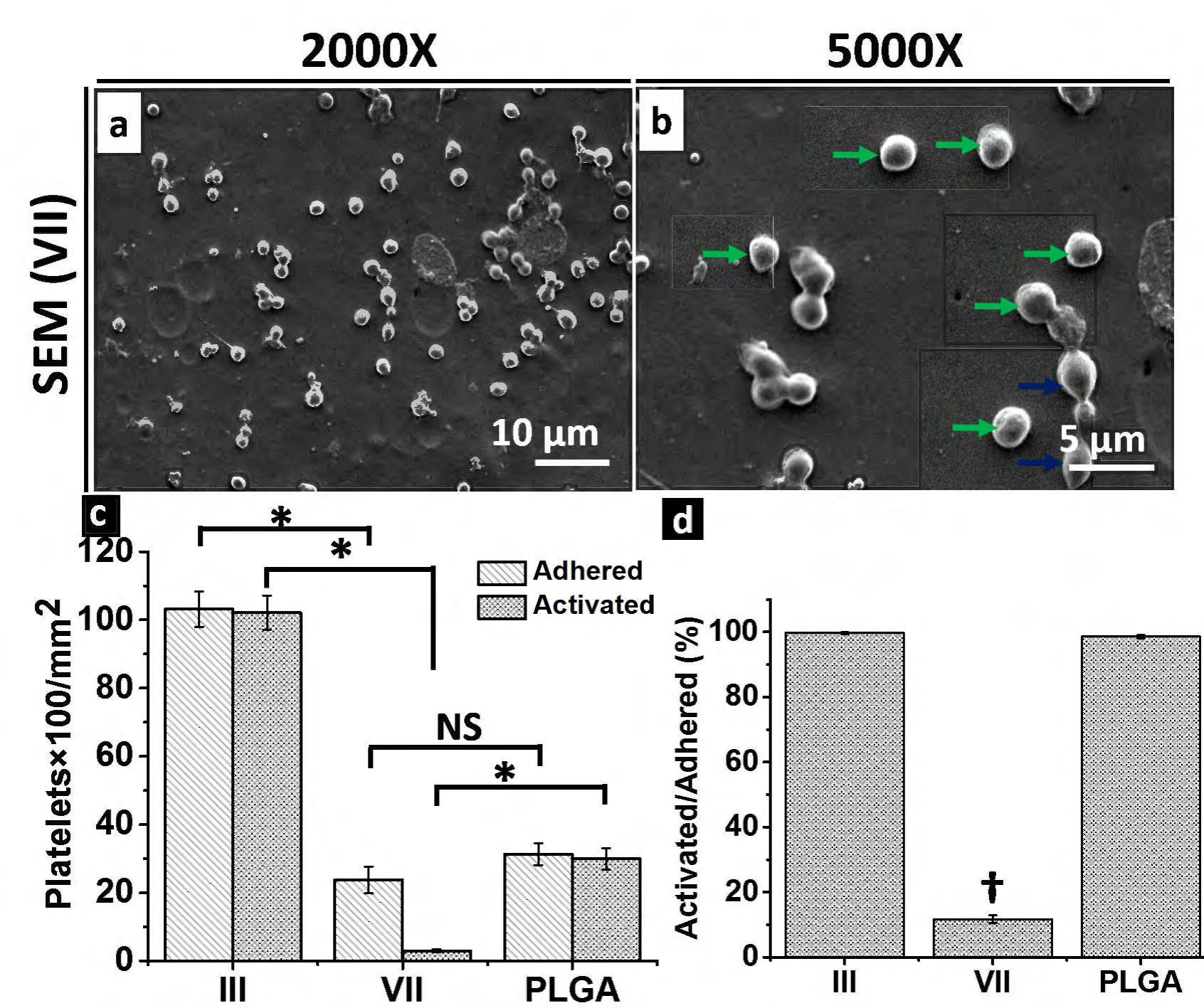
2000X
5000X
SEM (VII)
a
b
10 µm
5 µm
c
d
Platelets×100/mm2
Adhered
Activated
*
*
NS
*
120
100
80
60
40
20
0
III
VII
PLGA
Activated/Adhered (%)
†
100
80
60
40
20
0
III
VII
PLGA